SSC24-WVI-01

Radiation-Tolerant Ka-Band Deployable Phased-Array Transceiver for Low-Earth-Orbit Small Satellite Constellation

Yasuto Narukiyo, Xi Fu, Dongwon You, Sena Kato, Takashi Tomura, Hiraku Sakamoto, Kenichi Okada, Atsushi Shirane
2-12-1, Ookayama, Meguro-ku, Tokyo, 152-8552 Japan; +81-3-5734-3764
narukiyo.y.aa@ssc.pe.titech.ac.jp

ABSTRACT

This paper introduces the technology for radiation tolerance of Ka-band deployable phased-array antenna to provide wider communications infrastructure. Radiation in outer space degrades the performance of electronic devices. Furthermore, because the BFIC on the deployable phased-array antenna cannot be shielded due to the antenna structure, higher radiation tolerance is required than general aerospace ICs. The amount of radiation tolerance required was calculated and the high radiation tolerance technology of the BFIC was introduced, which was evaluated from the measurement results by exposing the BFIC to 3Mrad radiation which exceeds the conventional measurement dose.

1.INTRODUCTION

Recently, 5G communication, a high-frequency communication, has started, and further research is being conducted on 6G communication, which is an even higher frequency. However, high-frequency signals are difficult to spread over a wide area due to high spatial transmission loss and large signal attenuation caused by obstructions. In order to spread high-performance communication infrastructure over a wider area, the use of satellite constellations has been attracting attention in recent years. To realize satellite constellations, it is necessary to launch a large number of small satellites and to reduce launch costs, it is necessary to make satellites smaller. But as satellites become smaller, it becomes difficult to achieve high area antennas, and their performance as antennas deteriorate. To solve this problem, a deployable phased-array antenna is proposed. The deployable membrane structure enables the use of large antennas in space at low launch costs by downsizing the antenna at launch and deploying it after launch. The array antenna structure also makes it possible to send high-gain signals to targeted locations through phase control. Satellites equipped with these antennas will enable the use of high-frequency communications infrastructure anywhere on Earth.

In the future, we plan to build an array antenna and launch it into space to evaluate its performance. Figure 1 shows the structure of the CubeSat, a deployable phased-array antenna under design. The folded size of the satellite before launch is W6U (10cm x 20cm x 30cm), of which the folded array antenna is 2U (10cm x 20cm x 10cm). The membrane area in the deployed state is 67cm × 67cm after reaching space. The antenna area in the deployed membrane is 36cm x 36cm, and the other area is for heat dissipation. Although the proposed deployable phased-array antenna has a narrower signal transmission range than the horn antenna antennas used in [1] [2], it can compensate for this weakness by beamforming and can handle high-frequency signals. Furthermore, unlike the horn array antennas used in [3] [4], the deployable membrane structure makes it possible to reduce size and weight.

However, there are concerns about radiation effects on the beamforming integrated circuit (BFIC) used to control the phase of the signal when deployable phased-array antennas are used for satellite communications. While general space-use integrated circuits can be protected from radiation by covering them with metal shield such as aluminum, the complexity of the wiring on the deployable structure and the need to connect a large number of BFICs and a large number of antenna elements due to the array antenna structure make it difficult to place radiation shields between the BFIC and antenna elements. Therefore, the radiation tolerance of the BFIC itself must be higher than that of a general aerospace IC.

There are many papers that give a lot of radiation to transistors alone [5] [6]. However, there are few papers that give radiation to RF circuits for wireless communication [7] [8]. Among them, there are few papers on radiation tolerance of phased-array antennas exposing the entire phased-array antenna to radiation, not just the BFIC or papers that give radiation doses above 1Mrad.

This paper introduces the technology for radiation tolerance applied to the BFIC, as well as circuits to compensate for array antenna degradation by radiation. In addition, this paper shows the structure of the proposed BFIC and the prototype phased-array board with 64BFICs. At last, measurement results applying

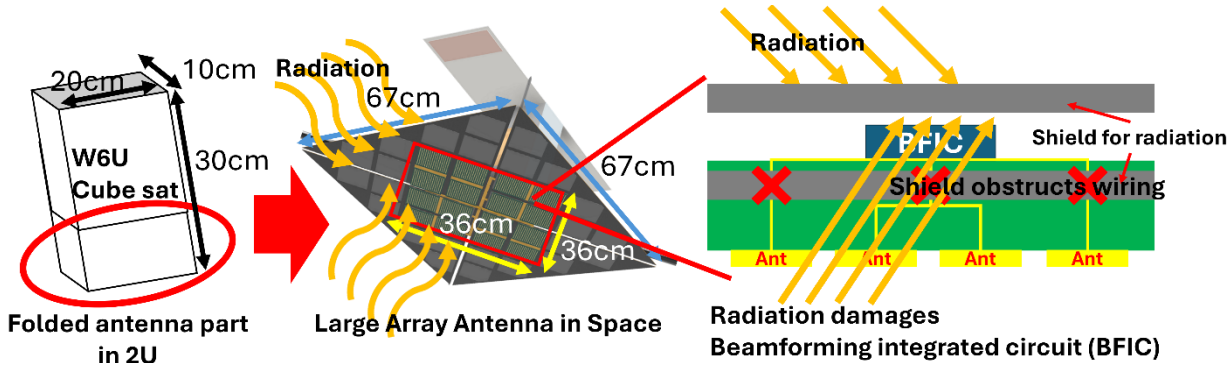

Figure 1: Structure of the deployable phased-array antenna and difficulty of shield for beamforming integrated circuit (BFIC)

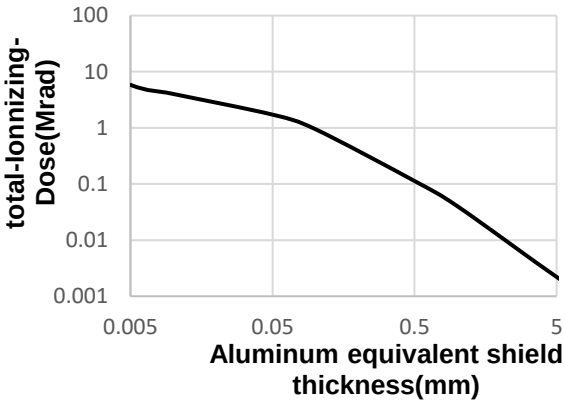

Figure 2: Total dose per aluminum equivalent shield thickness after 5 years at 550 km altitude

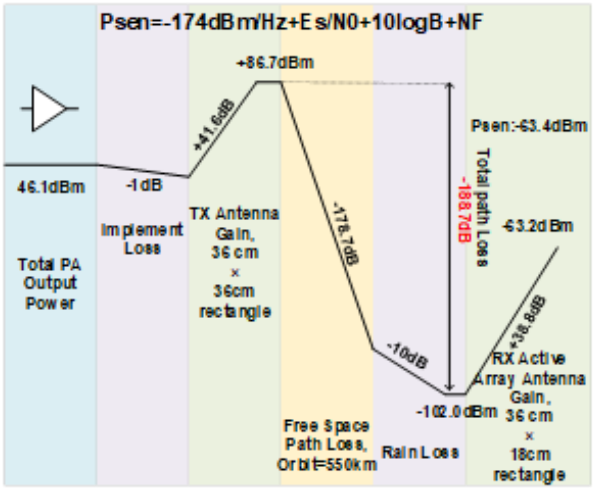

Figure 3: Link budget of the proposed antenna

Table 1: Shield thickness per antenna structure and Total dose

	horn antenna	Horn Array Antenna	planar phased array	Deployable Phased Array
Aluminum equivalent shield thickness	5mm or higher	5mm or higher	0.5mm or less	0.1mm or less
Total-Dose	2.4krad or less	2.4krad or less	110krad or higher	1.2Mrad or higher

radiation up to 3Mrad are introduced for showing stronger radiation tolerance than a conventional aerospace IC.

2.SYSTEM REQUIREMENTS

2.1 TID requirement

Figure 2 shows the results of the simulation using Spenvis [9]. The Total Ionizing Dose amount was calculated for a satellite in a sun-synchronous orbit at an altitude of 550 km for 5 years. Since the antenna part of the horn antenna and horn array antenna protrude from the board, it is easy to apply radiation shielding and to have a radiation shield of 5 mm or higher in aluminum equivalent. In antennas that cannot be radiation shielded, only the board is shielded, and in the case of a planar phased-array antenna, the aluminum equivalent shield thickness is about 0.5 mm or less. In the case of a deployable membrane phased-array antenna using a thinner substrate, the aluminum equivalent shield thickness is less than 0.1 mm or less. From Table 1, a radiation tolerance of more than 1.5Mrad is required for a deployable membrane phased-array antenna to be used for 5 years.

Table 2: Link budget of the proposed antenna in uplink

Frequency	29	GHz
PA output power: P_t	46.1	dBm
Received power: P_r	-63.2	dBm
Transmit antenna gain: G_t	41.6	dBi
Receive antenna gain: G_r	38.8	dBi
Space progation loss:L_{pass}	-178.7	dB
Sensitivity: P_{sen}	-63.4	dBm
Bandwidth	500	MHz
E_s/N_0	19.6	dB
Speed (256APSK)	4	Gbps

2.2 Communication Link Budget

Figure 3 and Table 2 show the results of the link budget calculations in uplink. In the proposed deployable membrane phased-array antenna, the receiver is half of the entire antenna surface. In this link budget calculation, G_r is calculated in this proposed antenna area. G_t was calculated assuming 35 cm square per side array antenna. P_t was calculated assuming a phased-array antenna that has 4096 antenna elements and outputs 10 dBm power from each antenna element. L_{pass}, which is the spatial propagation loss, was calculated assuming an altitude of 550 km. The amount of attenuation due to rain is assumed to be 10 dB. P_r is the sum of G_t, G_r, P_t and L_{pass}. P_{sen} was calculated assuming 4dB with NF, 19.6dB with E_s/N_0 of 256APSk, and the bandwidth of 500MHz. Since the value of P_r exceeds P_{sen}, it can be seen that the proposed antenna will allow a communication rate of 4 Gbps between an altitude of 550 km and the ground where the sky can be seen.

3.PROPOSED RADHARD PHAED-ARRAY

3.1 Receiver architecture

Figure 4 shows the antenna board equipped with 64IC and 256 antenna elements and a block diagram of the BFIC on the board [10]. This is a prototype of the proposed antenna, and the performance of the antenna was evaluated by measuring this. The signal received at the antenna patch first passes through the D-path. The phase is controlled by the phase-shifter, and the signal is

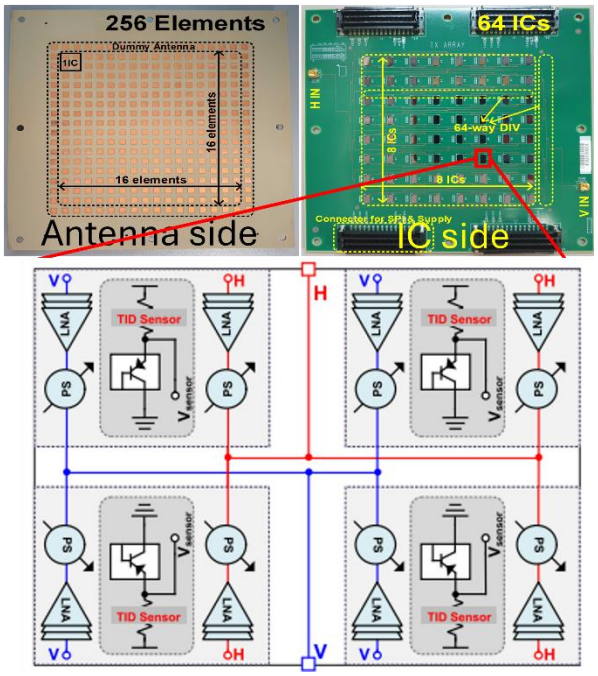

Figure 4: Prototype phased-array antenna and BFIC block diagram[10]

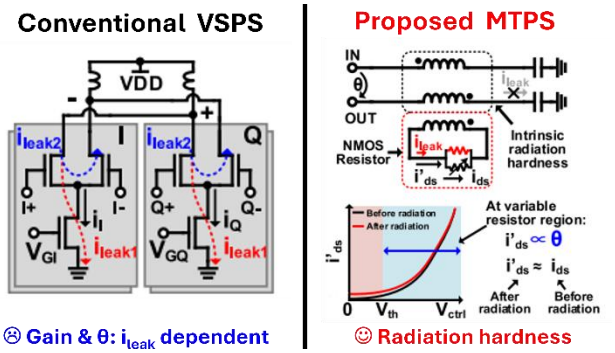

Figure 5: Comparison of phase-shifter architecture[12]

amplified by the LNA in the D-path. Next, it passes through the C-path and arrives at the microstrip line on the board. The phase and amplitude of the signal are adjusted by the phase-shifter, buffer, and VGA in the C-path. The receiver receives both horizontally and vertically polarized waves on the antenna element, which enables it to receive circularly polarized waves. Furthermore, by adjusting the phase with a phase-shifter, signals from any direction can be received. Additionally, TID sensors were installed inside all paths to detect the radiation dose. The IC was created by us in a 65nm CMOS process and packaged with wafer level chip scale package (WLCSP).

3.2 Phase-Shifter Architecture

Figure 5 shows the configuration of a conventional phase-shifter, and a radiation-tolerant phase-shifter proposed this time. In the conventional vector-summing

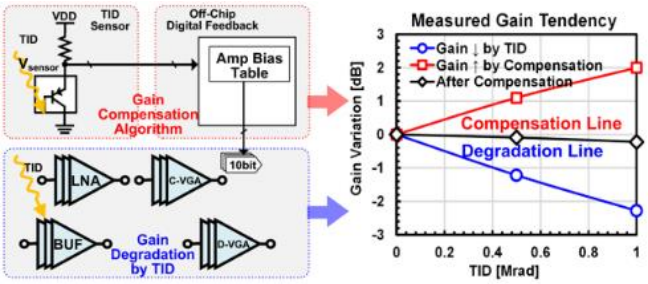

Figure 6: Structure of TID senser[10]

Modulation	16 APSK		
Symbol Rate	0.4 GBaud	0.8 GBaud	1.6 GBaud
Constellation*	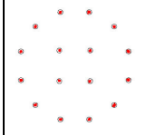	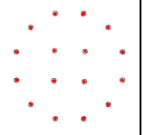	
Data Rate	1.6Gbps	3.2Gbps	6.4Gbps
RX EVM (RMS)	-38.2dB	-36.4dB	-33.1dB
Modulation	256 APSK		
Symbol Rate	0.4 GBaud	0.8 GBaud	1.6 GBaud
Constellation*		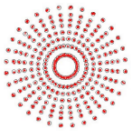	
Data Rate	3.2Gbps	6.4Gbps	12.8Gbps
RX EVM (RMS)	-37.7dB	-35.7dB	-33.2dB

Figure 7: OTA measurement results[12]

phase-shifter [11], TID induced leakage current leads to changes in phase and a gain reduction. Similarly, the performance of the passive phase-shifters along with varicap diodes for a fine-tuning function also decreases due to the same mechanism.

To address these issues, we designed a magnetic-tuning radiation-hardened phase-shifter [12]. The leakage current in the variable resistance region of the magnetic-tuning radiation-hardened phase-shifter is negligible, allowing the current from the drain to the source after radiation exposure to remain equal to that before exposure. By connecting three of this phase-shifter in succession, a phase of 180° can be covered. Furthermore, by inverting this phase with an amplifier, a phase of 360° can be covered.

3.3 TID senser

Figure 6 shows the structure of TID sensors for compensating the effect of TID. TID detection involves monitoring the dose of TID by detecting changes in the output voltage within the sensor. By applying a pre-set bias voltage to each amplifier based on the detected TID dose, it becomes possible to compensate for the TID impact on the IC. TID sensors can enhance the radiation tolerance of the entire phased-array system.

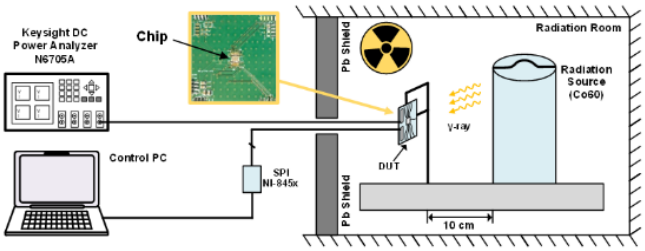

Figure 8: Proposed BFIC TID measurement setup[12]

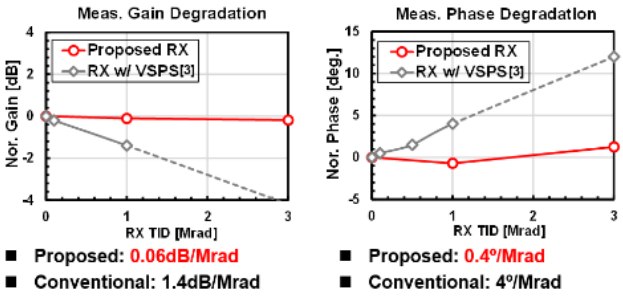

Figure 9: Measurement results of TID effect of the BFIC[12]

4.MEASUREMENT RESULTS

4.1 Prototype receiver OTA measurement results

Figure 7 shows the received signal constellation and EVMs of OTA (Over-The-Air) measurement results. The communication distance between the prototype receiver and the radiated horn antenna is 1.0 m. The horn antenna radiated 29GHz signal generated by a waveform generator. The signal was received by the prototype receiver with 64BFIC and then demodulated by an oscilloscope. The OTA EVMs are measured by 16APSK and 256APSK modulated signals with 0.4, 0.8, and 1.6GBaud signals. The prototype receiver can support 12.8Gbps with 256APSK at 29GHz signal. The power consumption of 1 antenna element is 3.4 mW. In addition, From the antenna gain and NF of the measurement result, the G/T of the prototype receiver is 11.5 dB/K.

4.2 Phase and Gain Variation by TID

The measurement setup is shown in Figure 8. In this measurement, the board with wire bonded BFIC with the proposed phase-shifter was irradiated up to 3Mrad while energized, and the phase shift was recorded simultaneously. Compared to [11], the gain reduction after 1Mrad irradiation was reduced to 0.06 dB, and the phase shift was significantly suppressed to 0.4°. Concerning the 5-year lifetime, the gain and phase reduction of the receiver are only 0.09 dB and 0.6°, respectively.

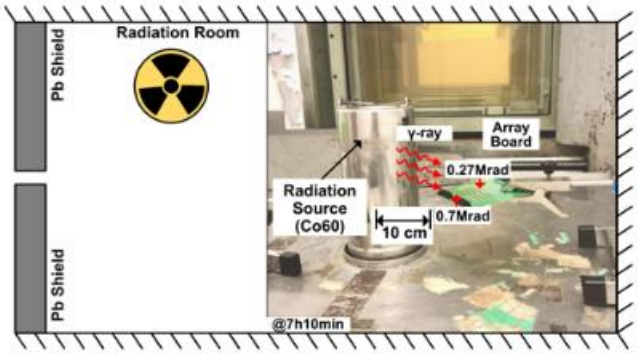

Figure 10: Phased-array TID measurement setup[10]

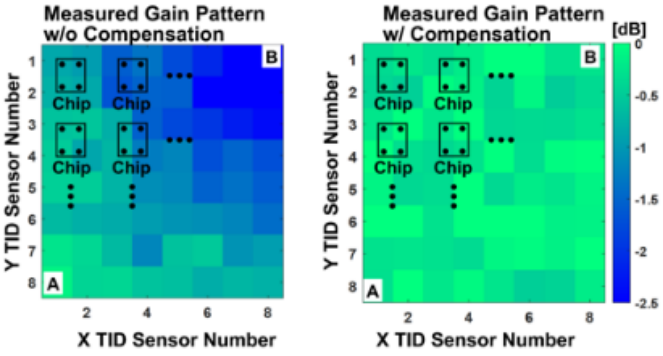

Figure 11: Measurement results of TID senser compensation[10]

Table 3: Comparison table

	Target @1Mrad	Proposed Transceiver @1Mrad	Conventional Transceiver [10] @1Mrad
Gain variation	-1dB	-0.06dB	-2.5dB
Worst Phase variation	1°	0.4°	6°

4.3 TID senser compensation

The measurement system is shown in Figure 10. The phased-array board was placed at an angle to the source so that all ICs present on the board with 16 ICs received different radiation doses. Furthermore, irradiation was performed until the average dose over the entire array surface reached 0.5Mrad, and then the measurement was performed.

Figure 11 shows the measurement results. Before compensation by TID sensor, the maximum value of gain difference between BFICs was 2.5 dB, but after compensation, the maximum value of the gain difference between BFICs was successfully reduced to 0.22 dB.

Table 4 shows the Comparison Table. This shows the radiation tolerance of the IC was greatly improved compared to the conventional IC [11].

5.CONCLUSION

Conclusion

This paper introduced radiation tolerance of the BFIC to be mounted on the antenna a deployable phased array antenna. From the measurement results, it was confirmed that the proposed BFIC has greater radiation tolerance compared to the conventional aerospace IC. By the radiation up to 3Mrad, the proposed BFIC gain, and phase variation can be reduced by 0.18dB and 0.4°. As a result, compared to conventional antenna ICs, it was possible to reduce the change in signal gain and beam angle even during a long-term stay in space.

Acknowledgments

This work is partially supported by NICT(JPJ012368C00601), MIC/SCOPE (192203002 and 192103003), JST A-STEP (JPMJTR211D), STAR, and VDEC in collaboration with Cadence Design Systems, Inc., Mentor Graphics, Inc., and Keysight Technologies Japan, Ltd.

References

1. S. Arora, V. S. Puram, B. S. Reddy, V. S. kumar, C. Sriharsha and D. V. Ramana, "X-band choked horn antenna for on-board TTC downlink of deep space satellite applications," *2017 IEEE International Conference on Antenna Innovations & Modern Technologies for Ground, Aircraft and Satellite Applications*, pp. 1-5, Nov. 2017.
2. U. Alkasi, "Placement Analysis of Isoflux Pattern Corrugated Horn Antenna on a Earth Observation Satellite Platform for LEO Altitude," *2023 7th International Electromagnetic Compatibility Conference*, pp. 1-6, Sep. 2023.
3. P. Kaith, M. M. Sharma, I. Sharma, I. B. Sharma, B. Kalra and Jaiverdhan, "8×1 Array Implementation of Bull's Horn Design Microstrip Patch Antenna for Broadcast Satellite and Military Communication," *2021 IEEE Indian Conference on Antennas and Propagation*, pp. 921-924, Dec. 2021.
4. M. Nagasaka, S. Nakazawa, M. Kamei, S. Tanaka and T. Ikeda, "Prototype of 32-element horn antenna array for imaging reflector antenna of 21-GHz band broadcasting satellite," *2014 11th European Radar Conference*, pp. 400-403, Oct. 2014
5. L. Cheva.s A. Nikolaus M. Bucher N. Makris A. Papadopoulou A. Zografos G. Borghello H.D. Koch F. Faccio, "Investigation of Scaling and Temperature Effects in Total Ionizing Dose (TID) Experiments in 65 nm CMOS," *2018 25th*

International Conference "Mixed Design of Integrated Circuits and System" (MIXDES), Gdynia, Poland, pp. 313-318, Jun. 2018

6. Y. Cao, W. De Cock, M. Steyaert and P. Leroux, "A 4.5 MGy TID-Tolerant CMOS Bandgap Reference Circuit Using a Dynamic Base Leakage Compensation Technique," in *IEEE Transactions on Nuclear Science*, vol. 60, no. 4, pp. 2819-2824, Aug. 2013.
7. A. Zanchi, M. Cabañas-Holmen, A. Amort and R. Brees, "Total Ionizing Dose Characterization of a Custom Front-End SoC for Antenna Arrays in 32nm SOI CMOS," *IEEE Radiation Effects Data Workshop*, pp. 1-7, Dec. 2018.
8. J. Budroweit and M. P. Jaksch, "In-Situ TID Testing and Characterization of a Highly Integrated RF Agile Transceiver for Multi-Band Radio Applications in a Radiation Environment," *IEEE International Conference on Wireless for Space and Extreme Environments*, pp. 1-6, Dec. 2019.
9. Spenvis https://www.spenvis.oma.be/
10. Xi Fu, Dongwon You, Xiaolin Wang , Yon Wang, Carolyn Jill Mayeda, Yuan Gan, Michiro Ide, Yuncheng Zhang, Jun Sakamaki, Ashibir Aviat Fadila, Zheng Li, Junpei Sudo, Makoto Higaki, Soichiro Inoue Takashi Eishima, Takashi Tomura, Jian Pang, Hiroyuki Sakai, Kenichi Okada, Atsushi Shirane, "A Low-Power 256-Element Ka-Band CMOS Phased-Array Receiver With On-Chip Distributed Radiation Sensors for Small Satellite Constellations," in *IEEE Journal of Solid-State Circuits*, vol. 58, no. 12, pp. 3380-3395, Dec. 2023.
11. A. Kawaguchi, J. Pang, Z. Li, K. Yanagisawa, A. Shirane and K. Okada, "Total Ionizing Dose Effects on 28GHz CMOS Bi-Directional Transceiver for 5G Non-Terrestrial Networks," 20th European Conference on Radiation and Its Effects on Components and Systems, pp. 1-4, Aug. 2020.
12. Xi Fu, Dongwon You, Yun Wang, Xiaolin Wang, Ashibir Aviat Fadila, Chenxin Liu, Sena Kato, Chun Wang, Zheng Li, Jian Pang, Atsushi Shirane, Kenichi Okada, "A Low-Power Radiation-Hardened Ka-Band CMOS Phased-Array Receiver for Small Satellite Constellation," in *IEEE Journal of Solid-State Circuits*, vol. 59, no. 2, pp. 349-363, Feb. 2024.